



ELASTIC BUCKLING OF CYLINDRICAL SHELLS WITH ELASTIC CORES—I. ANALYSIS

G. N. KARAM and L. J. GIBSON

Department of Civil and Environmental Engineering, Massachusetts Institute of Technology,
Cambridge, MA 02139, U.S.A.

Transmitted by John W. Hutchinson

(Received 14 February 1994; in revised form 10 June 1994)

Abstract—Thin walled cylindrical shell structures are widespread in nature; examples include plant stems, porcupine quills and hedgehog spines. All have an outer shell of almost fully dense material supported by a low density, cellular core. In nature, all are loaded in some combination of axial compression and bending; failure is typically by buckling. Natural structures are often optimized. Here we have analysed the elastic buckling of a thin cylindrical shell supported by an elastic core to show that this structural configuration achieves significant weight saving over a hollow cylinder. Biomimicking of natural cylindrical shell structures may offer the potential to increase the mechanical efficiency of engineering cylindrical shells. The results of the analysis are compared with data in the following companion paper.

NOTATION

<i>a</i>	radius to mid-plane of thickness
<i>b</i>	radius of bore hole
<i>c</i>	core thickness
<i>C</i>	curvature of cylinder in bending
<i>D</i>	flexural rigidity of shell = $Et^3/12(1-v^2)$
<i>E</i>	Young's modulus of shell
<i>E_c</i>	Young's modulus of core
<i>h</i>	$t/\sqrt{1-v^2}$
<i>I</i>	moment of inertia
<i>k_c</i>	spring constant for compliant core
<i>l</i>	length of shell
<i>l'</i>	half the buckling wavelength = l/m
<i>m</i>	longitudinal wave number
<i>M_{Brazier}</i>	Brazier moment
<i>M_{lb}</i>	local buckling moment
<i>N_x</i>	uniaxial compression per unit circumferential length
<i>P₀</i>	axial compressive buckling load of hollow shell
<i>P_{cr}</i>	axial compressive buckling load of shell with compliant core
<i>q</i>	uniform internal pressure inside shell
<i>t</i>	thickness of shell
<i>t_{eq}</i>	equivalent thickness of a hollow shell of equal mass and radius as shell with a compliant core
<i>u, v, w</i>	deformations along <i>x, y, z</i> directions
<i>U</i>	strain energy per unit length
<i>w_m</i>	maximum sinusoidal displacement in <i>z</i> direction
α	$[E_c/E]$
β	$(3-5v_c)/(1+v_c)(1-2v_c)$
β'	$v_c^2(5-2v_c)/(1+v_c)(1-2v_c)$
δ	maximum radial displacement under ovalization
ζ	degree of ovalization = δ/a
ζ_{cr}	degree of ovalization at $M_{Brazier}$
ζ_{lb}	degree of ovalization at local buckling
λ	buckling wavelength parameter = l'/π
λ_{cr}	value of λ minimizing N_x
<i>v</i>	Poisson's ratio of shell
<i>v_c</i>	Poisson's ratio of core

ρ	density of the shell
ρ_c	density of the core
σ_0	theoretical buckling stress in uniaxial compression of hollow shell
σ_{cr}	axisymmetric buckling stress of shell with compliant core under uniaxial compression
σ_{max}	maximum normal stress in bent cylinder
σ_z	stress in the z direction
$\frac{\sigma_z}{\sigma_z}$	normalized normal stress in z direction = $\sigma_z/\sigma_{z/z} = 0$
τ_{xz}	shear stress in the $x-z$ plane
$\bar{\tau}_{xz}$	normalized shear stress in $x-z$ plane = $\tau_{xz}/\tau_{xz/z} = 0$

1. INTRODUCTION

Thin walled cylindrical shell structures are widespread in nature; examples include plant stems, porcupine quills and hedgehog spines (Fig. 1). All have an outer shell of almost fully dense material supported by a low density, cellular core; biologists refer to this as a "core-rind" structure (Niklas, 1992). The cellular core can be made up of either foam-like cells (as in the parenchyma in the grass and hawthorne) or of a lattice of struts (as in the hedgehog spine). In nature, all of these structures are loaded in some combination of axial compression and bending; failure is typically by buckling. Natural structures are often optimized. The results of our analysis of the elastic buckling of a thin cylindrical shell supported by an elastic core, described below, suggest that this structural configuration achieves significant weight saving over a hollow cylinder.

Thin walled cylindrical shells are also widespread in engineering; examples include civil engineering structures, offshore oil platforms and aircraft fuselages. Ranges of the ratio of cylinder radius to wall thickness, a/t , for a variety of natural and engineering structures is shown in Fig. 2. In contrast to natural cylindrical shells which have a uniform, compliant core, engineering structures with large ratios of a/t are typically stiffened against buckling by circumferential and longitudinal members, known as ring stiffeners and stringers, respectively. Biomimicking of natural cylindrical shell structures may offer the potential to increase the mechanical efficiency of engineering cylindrical shells. As a first step in evaluating this possibility, we have analysed the elastic buckling of a cylindrical shell with a compliant core and compared its buckling resistance with that of a hollow cylindrical shell of equal mass. The results suggest that a compliant core significantly reduces the weight of a cylindrical shell. The results of the analysis are compared with data in the following, companion paper.

2. LITERATURE REVIEW

We first review the elastic buckling behaviour of a thin walled, hollow, cylindrical shell of radius a and wall thickness t , made of an isotropic material of Young's modulus E and Poisson's ratio v . In uniaxial compression, buckling takes place at a critical stress of (Timoshenko and Gere, 1961)

$$\sigma_0 = \frac{Et}{a\sqrt{3(1-v^2)}} \quad (1)$$

for any assumed buckling mode. Experimentally, it has been observed that thick, low modulus shells buckle axisymmetrically while thin, high modulus shells tend to buckle in a non-axisymmetric, diamond mode (Timoshenko and Gere, 1961; Kollár and Dulácska, 1984). In pure bending of infinitely long cylindrical shells, the circular cross-section ovalizes, reducing its moment of inertia. As the curvature is increased, the cross-section flattens up and the bending moment reaches a theoretical maximum, the Brazier moment (Brazier, 1927):

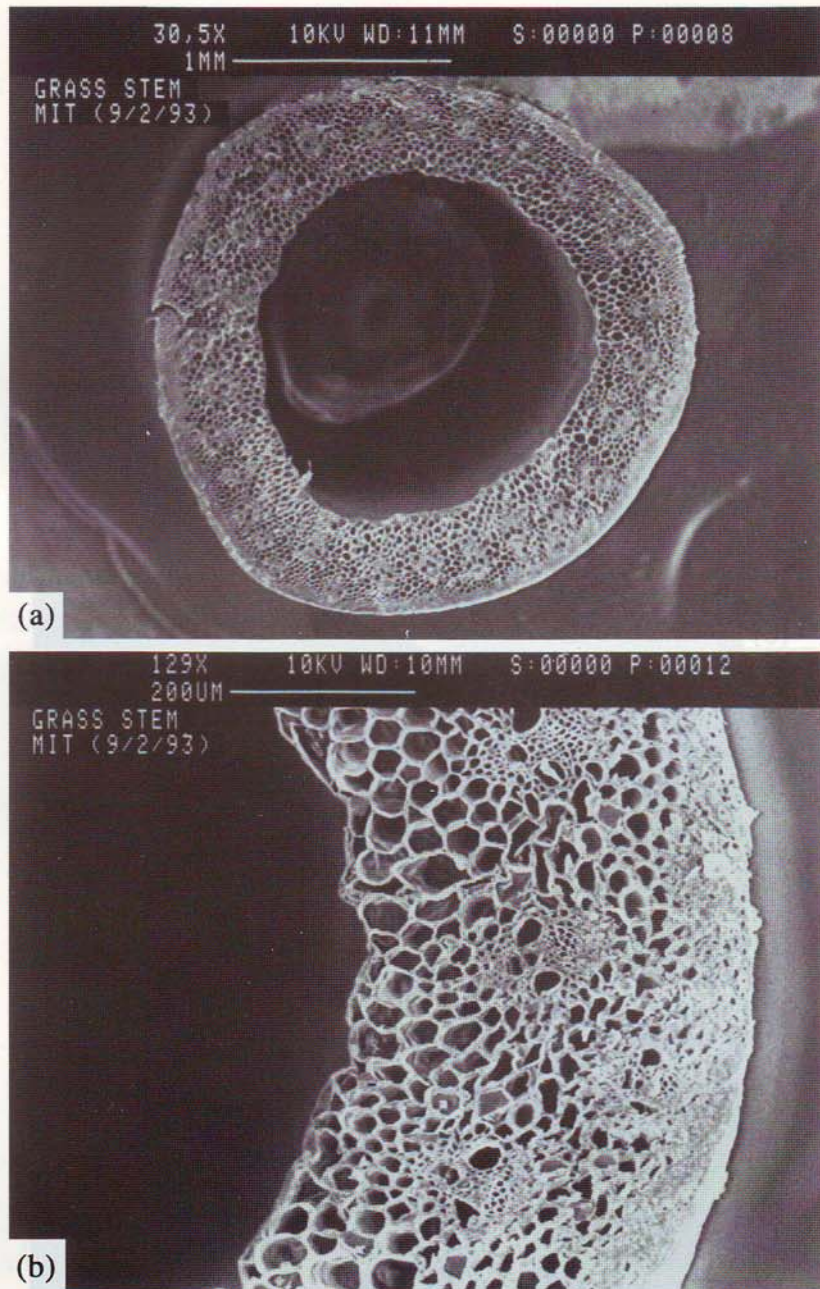
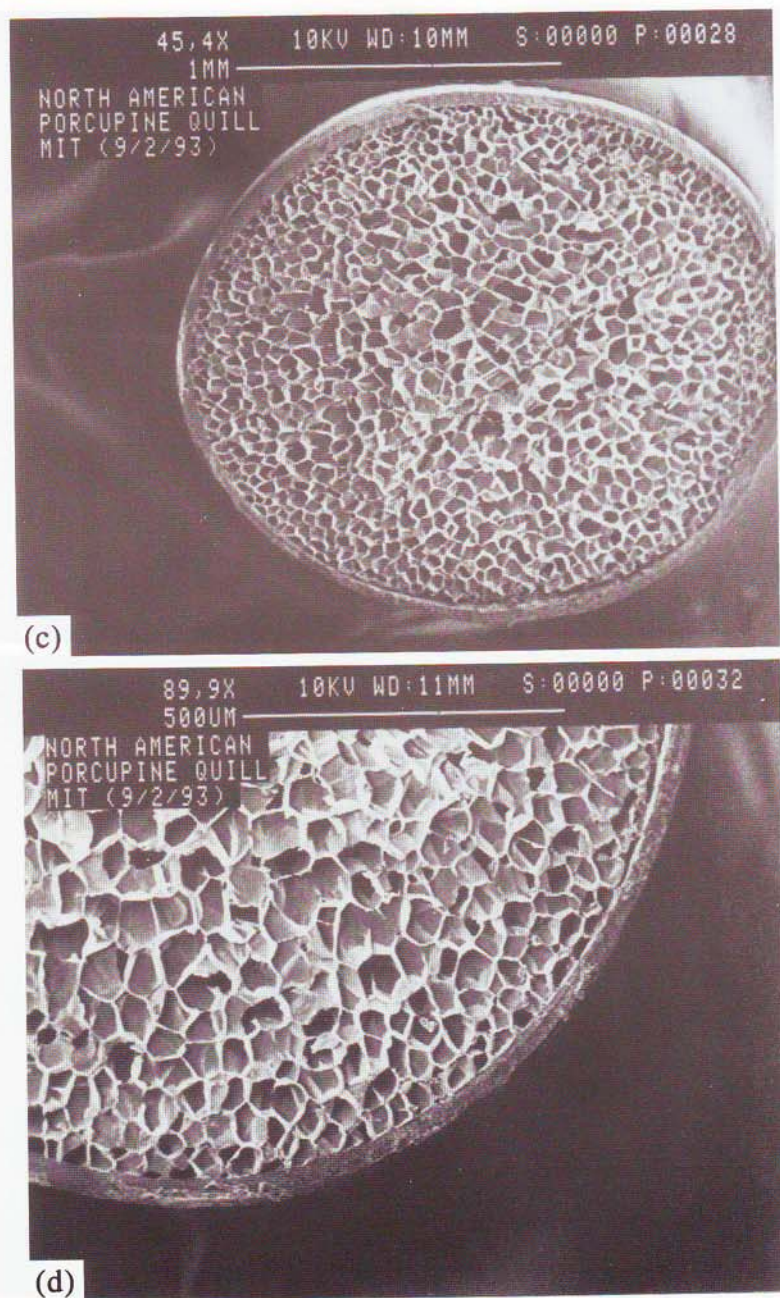
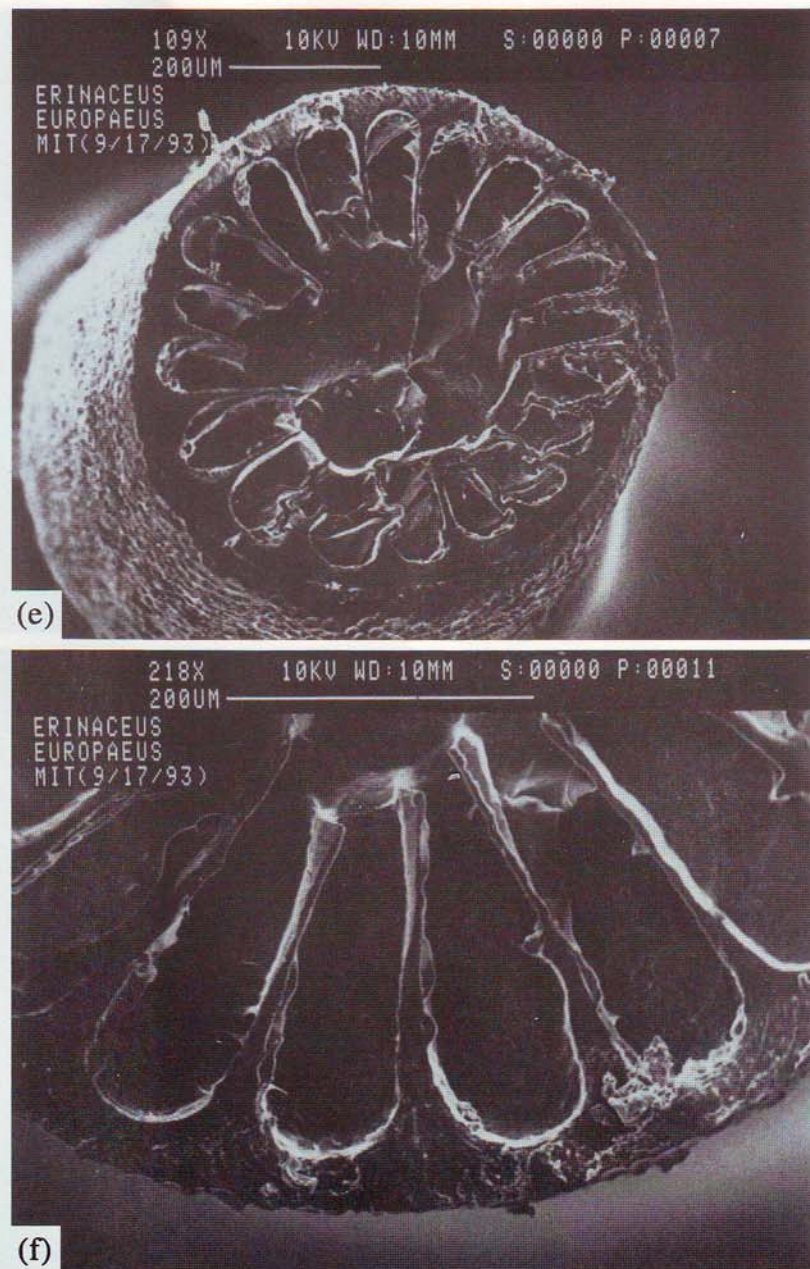
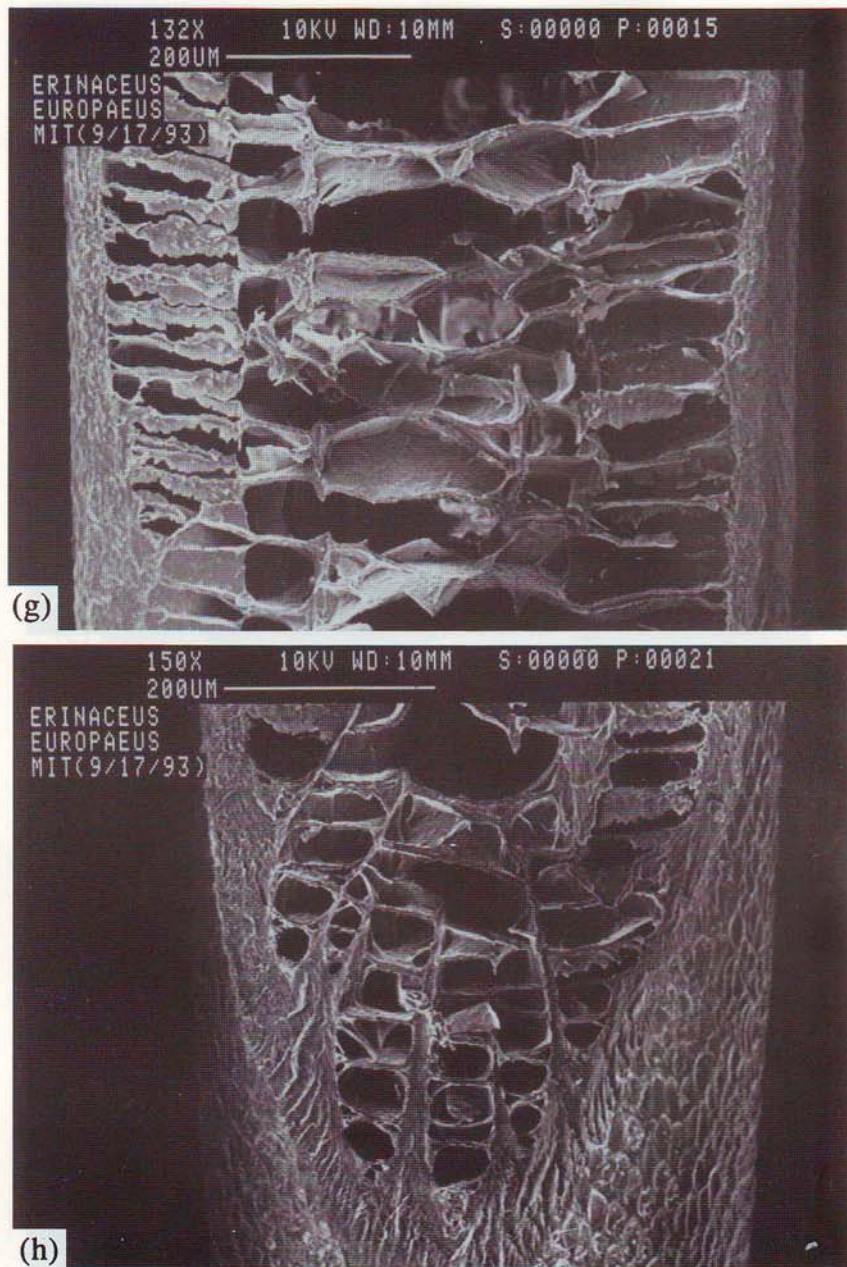


Fig. 1. Micrographs showing natural examples of cylindrical shells with compliant cores: (a, b) grass stem (*Elytrigia repens*); (c, d) North American porcupine (*Erethizon*) quill; (e-h) hedgehog (*Erinaceus europaeus*) spine. The grass and quill have a foam-like core while the spine has a more honeycomb-like latticed core.

Fig. 1. *Continued.*

Fig. 1. *Continued.*

Fig. 1. *Continued.*

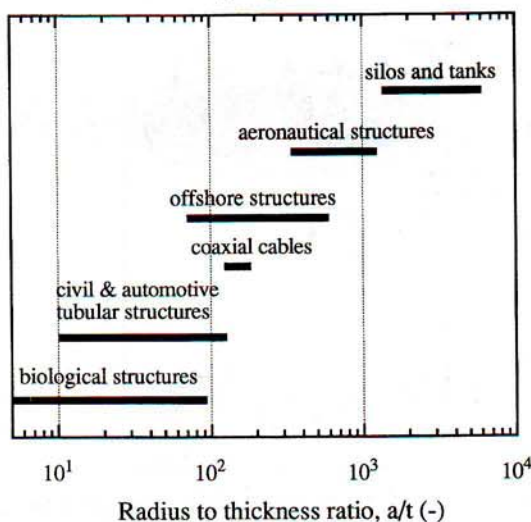


Fig. 2. Radius to thickness ratio a/t for natural and engineering cylindrical shells.

$$M_{\text{Brazier}} = \frac{2\sqrt{2\pi Eat^2}}{9\sqrt{1-v^2}} = \frac{0.987 Eat^2}{\sqrt{1-v^2}}. \quad (2)$$

In pure bending of short cylinders where ovalization is neglected, local buckling occurs when the stress on the compressive face of the shell reaches the critical stress to cause axisymmetric buckling under uniaxial compression [eqn (1)] (Seide and Weingarten, 1961). For an intermediate length shell the supports will hold the ends of the bent tube circular and hamper ovalization to some extent. The effects of length were first studied theoretically by Akselrad (1965). Stephens *et al.* (1975) investigated numerically the effect of length for four different specific geometries of thin walled circular tubes. Further investigations of the interaction between ovalization and bifurcation were performed by Fabian (1977), Reddy and Calladine (1978) and Gellin (1982). Calladine (1983) re-analysed the problem in terms of the geometric parameters of the shell; taking account of the ovalization of the cross-section for a long shell, he found that local buckling occurs at

$$M_{lb} = \frac{0.939 Eat^2}{\sqrt{1-v^2}}. \quad (3)$$

The moment required for local buckling is always lower than the Brazier moment.

The elastic buckling of a thin, isotropic cylindrical shell filled with a compliant elastic core has been analysed for a variety of loading configurations, including: axial load (Seide, 1962; Yao, 1962; Myint, 1966); uniform radial pressure (Seide and Weingarten, 1962; Seide, 1962; Herrmann and Forrestal, 1965); circumferential band of pressure (Yao, 1965); axial load plus uniform radial pressure (Seide, 1962; Brush and Almroth, 1962; Vlasov, 1972); axial load plus axially varying radial pressure (Brush and Almroth, 1962) or temperature (Zak and Bolland, 1962); axial load plus circumferential band of pressure (Brush and Almroth, 1962); and bending (Yabuta, 1980). More recently, the analysis has been extended to orthotropic cylindrical shells (Holston, 1967; Bert, 1971; Vlasov, 1975; Malyutin *et al.*, 1980) and to an elastic-plastic core (Babich and Cherevko, 1984). Natural cylindrical shell structures are typically loaded uniaxially and in bending; we consider the results for these two cases here.

The uniaxial load case has been solved by using the differential equations for equilibrium of the shell, modified to account for the spring constant of the compliant core (Seide, 1962) and by the use of stress functions (Yao, 1962). Both methods assume that the shell is thin and that the core modulus is lower than the shell modulus. Both treat the core as a three-dimensional solid and allow the core to be hollow. Furthermore, both methods

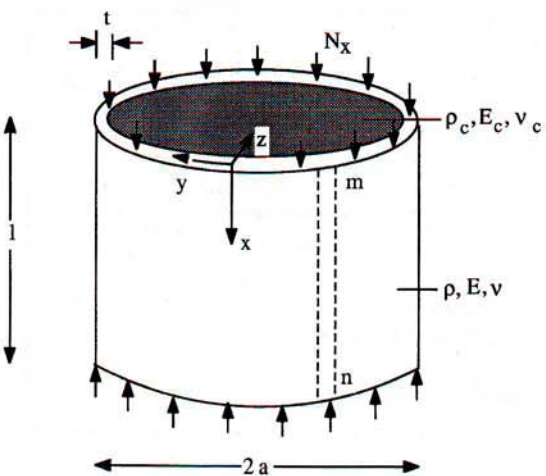


Fig. 3. A thin walled cylindrical shell with a compliant, elastic core.

allow for both longitudinal and circumferential buckling of the shell. The final results of both methods, which must be solved numerically, are similar and are consistent with finite element calculations (Weingarten and Wang, 1976). As expected, the buckling wavelength decreases and the buckling load increases, with increasing core stiffness. Seide (1962) notes that for a filled core the axisymmetric buckling mode gives the lowest buckling load.

Data for the uniaxial elastic buckling stress of cylinders with a compliant core lie significantly below Seide's (1962) estimates (Kachman, 1959; Fitzgibbon, 1960; Goree and Nash, 1962). A lower bound on the data is given by the minimum postbuckling load calculated by Almroth and Brush (1963). Observations of the buckling mode indicate that there is a transition between the classical diamond pattern for the empty cylinders to a circumferentially elongated diamond pattern in cylinders with a very low modulus core [$E_c/E = 3 \times 10^{-5}$ (Kachman, 1959)] to, finally, the axisymmetric mode in cylinders with a stiffer core [$E_c/E = 10^{-4}$ (Kachman, 1959)].

Local buckling arising from pure bending has been analysed by extending Seide's work and neglecting any ovalization of the cross-section (Yabuta, 1980). The relationships between the local buckling stress and E_c/E and a/t are plotted for a limited set of values. Bend tests were performed on four Mylar cylinders, two of which were empty and two of which were filled with silicone rubber ($E_c/E = 10^{-3}$). The empty and filled cylinders buckled at roughly 60% and 80% of the calculated load in a trend similar to that reported for the uniaxial load case.

Our goal is to compare the buckling resistance of cylindrical shells of equal mass with and without a compliant core for uniaxial compression, pure bending and combined compression and bending. We re-analyse the elastic buckling of a thin, isotropic cylindrical shell with a compliant elastic core to develop a simplified, more tractable analysis for axisymmetric buckling in uniaxial compression and for the ovalization, Brazier moment and local buckling moment in pure bending. We then compare the buckling resistance of hollow cylindrical shells to that of cylindrical shells with a compliant core to evaluate mechanical efficiency. Finally, we describe the potential for biomimicking of natural cylindrical shells in engineering design.

3. ANALYSIS

3.1. Axial compression—axisymmetric buckling

A circular cylindrical shell of radius a and wall thickness t , with a compliant elastic core, is shown in Fig. 3. The shell has a density ρ , a Young's modulus E and a Poisson's ratio v ; the core has a density ρ_c , a Young's modulus E_c and a Poisson's ratio v_c . We define coordinate x , y and z axes as shown with corresponding deformations u , v and w . We calculate the critical stress for axisymmetric elastic buckling under uniaxial compression by

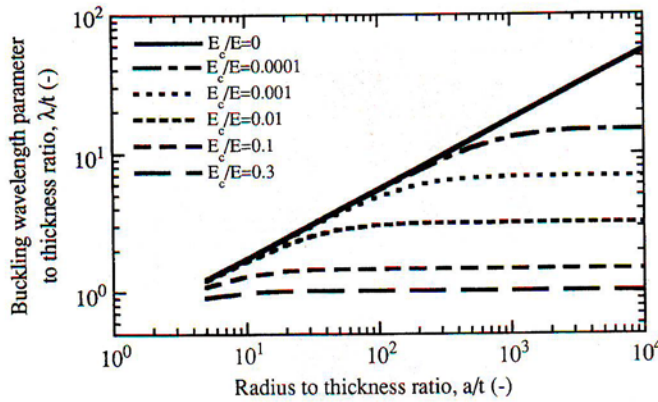


Fig. 4. The normalized axisymmetric buckling wavelength parameter λ/t for a cylindrical shell plotted against radius to thickness ratio a/t for various values of E_c/E . Each curve can be approximated by a bilinear relationship. λ is the buckling half wavelength divided by π .

modifying Timoshenko and Gere's (1961) results for the symmetric deformation and axisymmetric buckling of a hollow cylindrical shell to account for the compliant core as a two-dimensional elastic foundation stabilizing a longitudinal strip mn of the shell (Fig. 3). We assume a sinusoidal radial displacement during buckling given by

$$w = w_m \sin\left(\frac{m\pi x}{l'}\right) \quad (4)$$

where l' , the half buckled wavelength, equals l/m . The compliant core or foundation is treated as a half elastic space with a spring constant k_e given by (Gough *et al.*, 1940; Allen, 1969)

$$k_e = \frac{2E_c}{(3-v_c)(1+v_c)} \frac{1}{\lambda} \quad (5)$$

where $\lambda = l/m\pi = l'/\pi$.

The axial load N_x in the buckled shell strip mn is then given by

$$N_x = D \frac{1}{\lambda^2} + \frac{Et}{a^2} \lambda^2 + \frac{2E\alpha\lambda}{(3-v_c)(1+v_c)} \quad (6)$$

with $D = Et^3/12(1-v^2)$ and $\alpha = E_c/E$.

The minimum buckling load is found by setting the derivative of N_x in eqn (6), with respect to λ , equal to zero. The root λ_{cr} can be solved by using a numerical procedure such as Newton-Raphson for given values of a , t , α and E ; it is plotted in Fig. 4. Note that for $(a/t)^2 (E_c/E) < 0.1$, λ_{cr} is given by the result for an empty cylinder:

$$\frac{\lambda_{cr}}{t} = \frac{1}{[12(1-v^2)]^{1/4}} \left(\frac{a}{t}\right)^{1/2}. \quad (7)$$

For $(a/t) (E_c/E) > 10$, λ_{cr} is given by the result for wrinkling of a flat sheet on an elastic foundation (Allen, 1969):

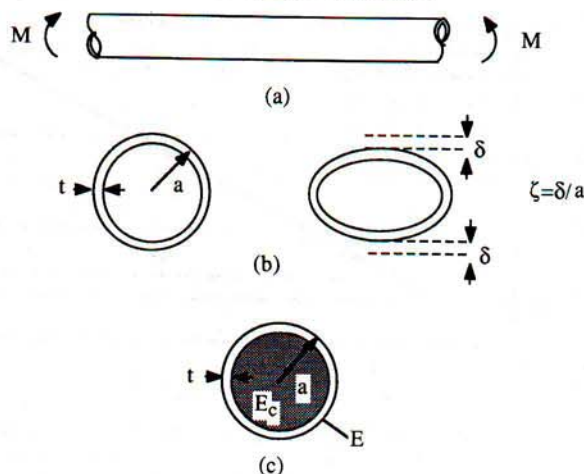


Fig. 5. (a) A hollow cylindrical shell in pure bending. (b) Ovalization of the initially circular cross-section. The degree of ovalization is $\zeta = \delta/a$. (c) A cylindrical shell of modulus E filled with a compliant core of modulus E_c .

$$\frac{\lambda_{cr}}{t} = \left[\frac{(3-v_c)(1+v_c)}{12(1-v^2)} \right]^{1/3} \left[\frac{E}{E_c} \right]^{1/3}. \quad (8)$$

The critical buckling stress can then be found from eqn (6). Alternatively, noting that $\sigma_{cr} = N_x/t$ and $D = Et^3/12(1-v^2)$, we can write the critical buckling stress in the shell as

$$\sigma_{cr} = \sqrt{3(1-v^2)}\sigma_0 f_1 \quad (9)$$

where

$$f_1 = \frac{1}{12(1-v^2)} \frac{a/t}{(\lambda_{cr}/t)^2} + \frac{(\lambda_{cr}/t)^2}{a/t} + \frac{2\alpha}{(3-v_c)(1+v_c)} (\lambda_{cr}/t)(a/t)$$

and where σ_0 is the buckling stress for the hollow cylinder [eqn (1)]. The total axial buckling load P_{cr} , found by assuming that the core has to deform along with the shell in compression prior to buckling, and neglecting any other interaction prior to buckling, is then

$$P_{cr} = 2\pi a t \sigma_{cr} \left(1 + \frac{a}{2t} \frac{E_c}{E} \right). \quad (10)$$

3.2. Pure bending—the Brazier effect

In pure bending, the cross-section of a hollow cylindrical shell *ovalizes*, decreasing the moment of inertia and flexural rigidity of the section (Fig. 5). The moment carrying capacity of the cross-section reaches a maximum at the *Brazier* moment $M_{Brazier}$ given by eqn (2) for a hollow cylinder. The *Brazier* moment of a cylindrical shell filled with a compliant core can be calculated by writing the strain energy per unit length U of the cylinder in terms of the curvature C and the degree of ovalization ζ , noting that for a given curvature the degree of ovalization is that which minimizes strain energy (i.e. $dU/d\zeta = 0$) and finding the maximum moment by taking $dU/dC = 0$. For a cylindrical shell filled with a compliant core, the strain energy is composed of the longitudinal stretching and the circumferential bending strain energies of the shell to which the energy of ovalization of a circular disk of foam core and the energy to counter Poisson's effects due to bending of the foam core are added. The moment of inertia of the cross-section is also increased by the presence of the compliant core. Each of these effects is calculated in the Appendix. The final result for the strain energy of the cylindrical shell with a compliant core is

$$U = \frac{1}{2} C^2 E \pi a^3 t \left(1 + \frac{\alpha a}{4t} \right) \left(1 - \frac{3}{2} \zeta + \frac{5}{8} \zeta^2 \right) + \frac{3}{8} \pi E \frac{t}{a} h^2 \zeta^2 + \frac{\pi}{4} \alpha \beta E \zeta^2 a^2 + \frac{\pi}{16} \alpha \beta' E C^2 a^4 \quad (11)$$

where

$$\alpha = E_c/E, \quad h = \frac{t}{\sqrt{1-v^2}}, \quad \text{and} \quad \zeta = \delta/a$$

$$\beta = \frac{3-5v_c}{(1+v_c)(1-2v_c)} \quad \text{and} \quad \beta' = \frac{v_c^2(5-2v_c)}{(1+v_c)(1-2v_c)}.$$

For a given curvature C the ovalization that minimizes strain energy is [neglecting the term $5/8 \zeta^2$ in eqn (11)]

$$\zeta = C^2 \frac{a^4}{h^2} \left(\frac{1 + \frac{\alpha a}{4t}}{1 + \frac{2}{3} \alpha \beta \frac{a^3}{th^2}} \right). \quad (12)$$

Substituting this value in eqn (11) and taking $\partial^2 U / \partial C^2 = \partial M / \partial C = 0$, we obtain the Brazier moment:

$$M_{\text{Brazier}} = \frac{2\sqrt{2}}{9} \pi E a t h \left(1 + \frac{2}{3} \alpha \beta \frac{a^3}{th^2} \right)^{1/2} \left(1 + \frac{\alpha a}{4t} + \frac{\alpha \beta' a}{8t} \right)^{3/2} \left(1 + \frac{\alpha a}{4t} \right)^{-1}. \quad (13)$$

At the Brazier moment the ovalization is

$$\zeta_{\text{cr}} = \frac{2}{9} \left[1 + \frac{\alpha \beta' \frac{a}{8t}}{\left(1 + \frac{\alpha a}{4t} \right)} \right]. \quad (14)$$

The maximum compressive stress in the shell at the Brazier moment is

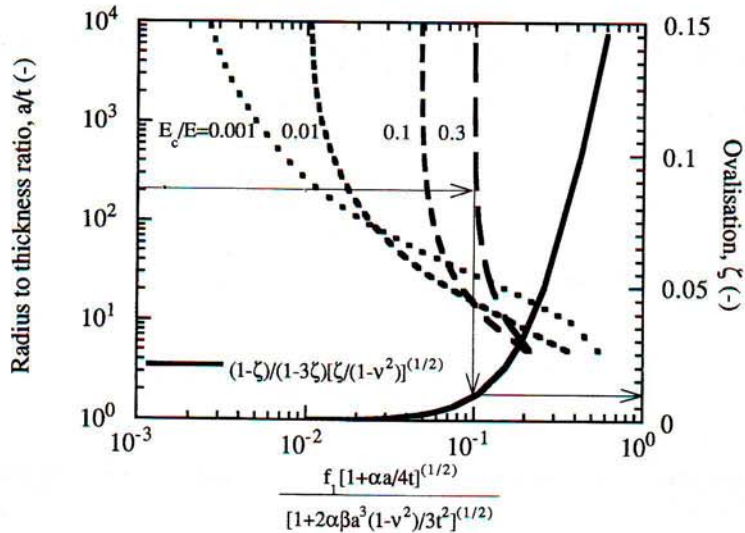
$$\sigma_{\max} = E C a (1 - \zeta_{\text{cr}}); \quad (15)$$

at the Brazier moment it is also

$$\sigma_{\max} = \frac{Et}{a \sqrt{1-v^2}} (\zeta_{\text{cr}})^{1/2} (1 - \zeta_{\text{cr}}) \frac{\left(1 + \frac{2 \alpha \beta a^3 (1-v^2)}{3t^3} \right)^{1/2}}{\left(1 + \frac{\alpha a}{4t} \right)^{1/2}}. \quad (16)$$

3.3. Pure bending—local buckling

True local buckling corresponding to a bifurcation point occurs if the normal stress in the compressive side of the cylindrical shell reaches the critical stress for axisymmetric buckling calculated above [eqn (9)]. Following Calladine's analysis for an empty cylindrical shell we observe that (Calladine, 1983)

Fig. 6. Nomograph for solution of ζ_{lb} for a cylindrical shell with compliant core.

$$\sigma_{\max} = \sigma_{cr}(1 - 3\zeta) \quad (17)$$

where σ_{cr} is the uniaxial compressive stress for axisymmetric buckling. By substituting eqns (9), (12) and (15), we obtain

$$\frac{\zeta^{1/2}(1-\zeta)}{\sqrt{1-v^2}(1-3\zeta)} = f_1 \frac{\left(1 + \frac{\alpha a}{4t}\right)^{1/2}}{\left[1 + \frac{2\alpha\beta a^3(1-v^2)}{3t^2}\right]^{1/2}}. \quad (18)$$

which can be solved numerically for the ovalization at which local buckling occurs, ζ_{lb} , or by using the nomograph in Fig. 6. The critical moment for local buckling is found by substituting the result of eqn (18) in eqns (11) and (12) and writing $M = \partial U / \partial C$. By writing the moment in terms of the ovalization at which local buckling occurs, we obtain

$$M_{lb} = \frac{\pi Eat^2 \sqrt{\zeta_{lb}}}{\sqrt{1-v^2}} \left(1 + \frac{\frac{\alpha\beta'a}{8t}}{1 + \frac{\alpha a}{4t}} - \frac{3}{2}\zeta_{lb} \right) \left(1 + \frac{2\alpha\beta a^3}{3t^2} \right)^{1/2} \left(1 + \frac{\alpha a}{4t} \right)^{1/2}. \quad (19)$$

The moment to cause local buckling is always lower than the Brazier moment.

3.4. Combined axial load and bending moment

Local buckling can also take place under the combined action of an axial load P and a bending moment M . The combined load at any section of the core filled cylinder can be replaced by an axial load applied with an eccentricity e , with respect to the axis of the cylinder, with $M = Pe$. Local buckling will take place when the maximum compressive stress in the shell reaches the axisymmetric axial compression buckling stress. The maximum compressive stress is the sum of the stress due to the axial load and that due to bending. Noting that the curvature is given by $C = M/EI$, and replacing M and I by their values, we find

$$C = \frac{Pe}{\pi E a^3 t \left(1 - \frac{3}{2} \zeta\right) \left(1 + \frac{\alpha a}{4t}\right)}. \quad (20)$$

Using eqn (12) the ovalization can be solved numerically from

$$\zeta \left(1 - \frac{3}{2} \zeta\right)^2 = \left(\frac{Pe}{\pi E a h}\right)^2 \frac{1}{\left(1 + \frac{\alpha a}{4t}\right) \left(1 + \frac{2\alpha \beta a^3}{3t h^2}\right)}. \quad (21)$$

The stress due to bending is

$$\sigma_{\text{bending}} = \frac{Pe a (1 - \zeta)}{\pi a^3 t \left(1 - \frac{3}{2} \zeta\right) \left(1 + \frac{\alpha a}{4t}\right)} \quad (22a)$$

and that due to axial compression is

$$\sigma_{\text{axial}} = \frac{P}{2\pi a t \left(1 + \frac{\alpha a}{2t}\right)}. \quad (22b)$$

Summing the two stresses, equating them to the axisymmetric buckling stress [eqn (9)] and solving for P , we get

$$P_{\text{cr}} = \frac{\frac{Et}{a} (1 - 3\zeta) f_1}{\frac{ea (1 - \zeta)}{\pi a^3 t \left(1 - \frac{3}{2} \zeta\right) \left(1 + \frac{\alpha a}{4t}\right)} + \frac{1}{2\pi a t \left(1 + \frac{\alpha a}{2t}\right)}}. \quad (23)$$

For a given eccentricity e , this equation can be solved for the critical axial load P_{cr} . Conversely, given the load P_{cr} , the maximum eccentricity can be obtained by simultaneously solving eqn (21).

3.5. Stress decay within the core

The buckling analyses described above treat the core as an elastic foundation resisting buckling of the shell. The normal σ_z and shear τ_{xz} stresses developed in the core are maximum at the interface between the shell and the core ($z = 0$) and decay within the core with increasing z . The decay of these stresses within the core can be closely approximated using the solution for a buckled flat strip supported by an elastic half-space (Fig. 7) (Allen, 1969). Normalizing σ_z and τ_{xz} by $\sigma_z(z = 0)$ and $\tau_{xz}(z = 0)$, respectively, we obtain

$$\bar{\sigma}_z = \frac{\sigma_z}{\sigma_{z/z=0}} = \left[1 + \left(\frac{1+v_c}{2}\right) \frac{\pi z}{l'}\right] \exp\left(-\frac{\pi z}{l'}\right) \quad (24a)$$

and

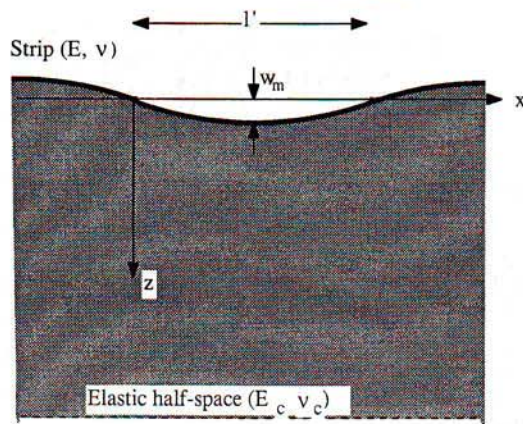
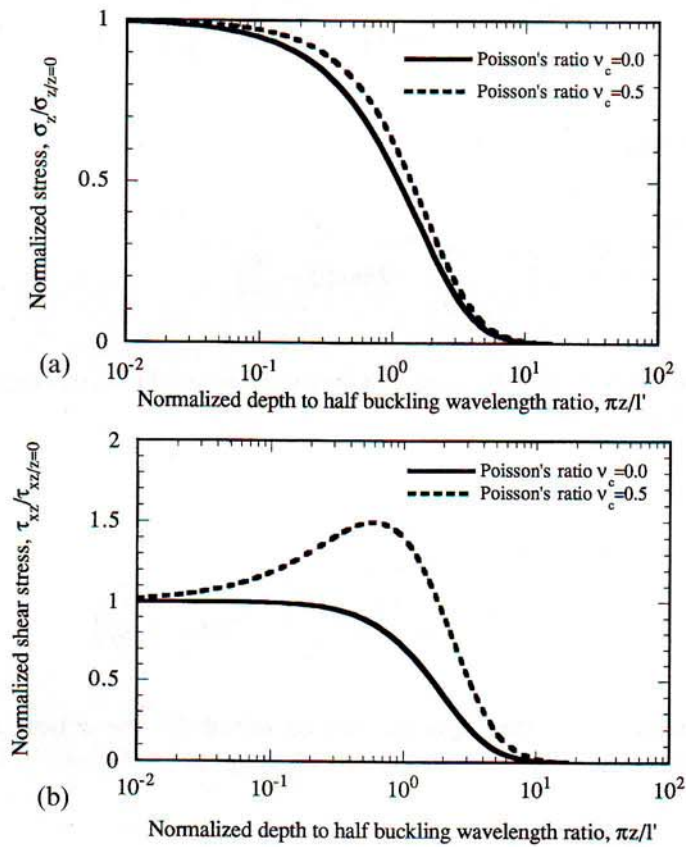


Fig. 7. A buckled flat strip on an elastic half-space.

Fig. 8. (a) Decay of normal stress in the z direction with depth into the core z ; (b) decay of shear stress in the $x-z$ plane with depth into the core z .

$$\bar{\tau}_{xz} = \frac{\tau_{xz}}{\tau_{xz/z=0}} = \left[1 + \left(\frac{1+v_c}{1-v_c} \right) \frac{\pi z}{l'} \right] \exp \left(- \frac{\pi z}{l'} \right). \quad (24b)$$

Both stresses are plotted as a function of $(\pi z/l')$ in Fig. 8, for $v_c = 0$ and $v_c = 0.5$. We observe that the stresses decay to about 5% of their maximum value at $\pi z/l' = 5$, or at a depth of 1.6 half wavelengths. Similar results are found for a strip supported by an elastic foundation of finite thickness. Core material at $z > 1.6 l'$ does not resist any load and can be removed without reducing the axisymmetric buckling stress in uniaxial compression or the local buckling stress in bending.

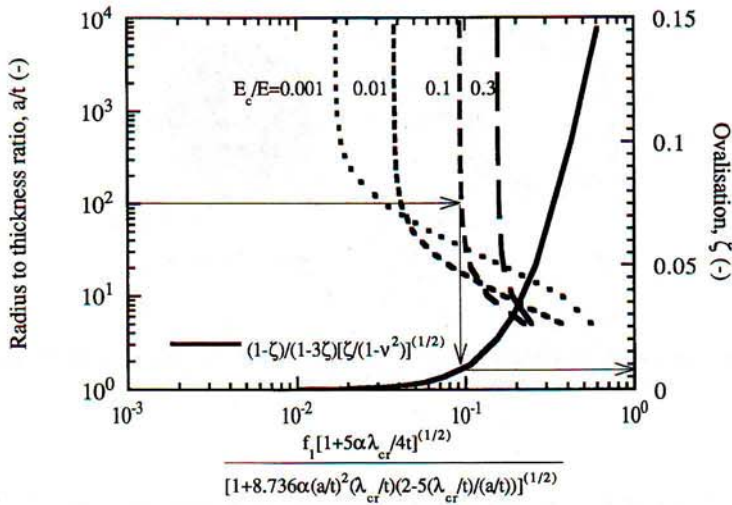


Fig. 9. Nomograph for solution of ζ_{lb} for a cylindrical shell with compliant core with central bore hole.

The buckling resistance of the cylindrical shell with a compliant core of thickness $c \geq 1.6t$ and with a central bore hole of radius b is obtained by modifying the previous results. The uniaxial compressive stress at which axisymmetric buckling occurs remains unchanged. The Brazier moment is modified as follows. The moment of inertia of the cross-section becomes

$$I = \pi a^3 t + \frac{E_c}{E} \frac{\pi a^4}{4} \left(1 - \frac{b^4}{a^4} \right).$$

Setting $b = a - c$ and $c = 5\lambda$ gives

$$I = \pi a^3 t \left[1 + \frac{E_c}{E} \frac{a}{4t} \left\{ 1 - \left(1 - \frac{5\lambda_{cr}/t}{a/t} \right)^4 \right\} \right]. \quad (25)$$

The strain energy of ovalization for the core becomes

$$U = \frac{\pi}{4} \alpha \beta E \zeta^2 (a^2 - b^2) = \frac{\pi}{4} \alpha \beta E \zeta^2 a^2 \left[1 - \left(1 - \frac{5\lambda_{cr}/t}{a/t} \right)^2 \right] \quad (26)$$

and the strain energy due to Poisson's effect becomes

$$U = \frac{\pi}{16} \alpha \beta' E C^2 a^4 \left(1 - \frac{b^4}{a^4} \right) = \frac{\pi}{16} \alpha \beta' E C^2 a^4 \left[1 - \left(1 - \frac{5\lambda_{cr}/t}{a/t} \right)^4 \right]. \quad (27)$$

The moment at which local buckling moment occurs is found, as before, by setting the moment equal to the derivative of the strain energy with respect to curvature, using the ovalization at which local buckling occurs. The procedure is identical to the previous analysis with the strain energy of the core modified by eqns (25), (26) and (27). The ovalization at which local buckling occurs is given by the solution to

$$\sqrt{\frac{\zeta}{1-v^2}} \frac{1-\zeta}{1-3\zeta} = f_1 \frac{\left(1 + \frac{5}{4} \frac{E_c}{E} \frac{\lambda_{cr}}{t} \right)}{\left[1 + 8.74 \left(\frac{a}{t} \right)^2 \frac{E_c}{E} \frac{\lambda_{cr}}{t} \left(2 - 5 \frac{\lambda_{cr}/t}{a/t} \right) \right]^{1/2}}. \quad (28)$$

The solution can be found numerically or by using the nomograph in Fig. 9 (for

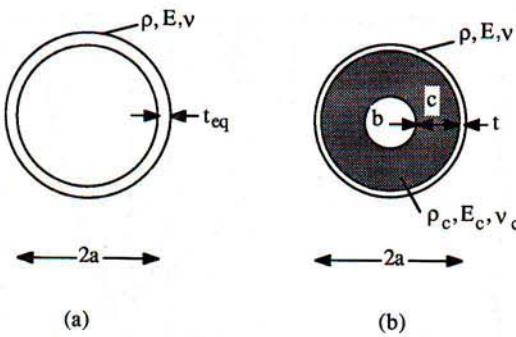


Fig. 10(a). Thin walled cylindrical shell (no core); (b) thin walled cylindrical shell with a compliant core of depth c of equal radius and mass as shell in (a).

$v = v_c = 0.3$). The moment at which local buckling occurs is then given by eqn (19) using the value of $\zeta = \zeta_{lb}$ that satisfies the above equation and the modifications given in eqns (25)–(27).

3.6. Combined buckling of shell and core

The above analysis for the stress decay within the core assumes that the core continues to function as an elastic foundation. In practice, if the core thickness is sufficiently reduced, the core will deform sinusoidally, as a unit, along with the shell. The buckling load is that given for a hollow cylinder by Timoshenko and Gere (1961), with D and t replaced by values for the transformed section D' and t' . The moment of inertia for a unit circumferential length of shell and core is

$$I = \left(\frac{\alpha^3 c^3 + t^3}{12} \right) + t \left(c + \frac{t}{2} - y_0 \right)^2 + \alpha c \left(y_0 - \frac{c}{2} \right)^2$$

giving the equivalent bending rigidity of the section as

$$D' = \left(\frac{E}{1-v^2} \right) \left[\left(\frac{\alpha^3 c^3 + t^3}{12} \right) + t \left(c + \frac{t}{2} - y_0 \right)^2 + \alpha c \left(y_0 - \frac{c}{2} \right)^2 \right]$$

where y_0 is the location of the centroid of the section measured from the free face of the core, and $v_c = v$. The equivalent thickness of the section is

$$t' = t + \alpha c.$$

The generalized buckling stress is then

$$\sigma_{cr} = \frac{2}{at'} \sqrt{ED't'}. \quad (29)$$

4. COMPARISON OF BUCKLING RESISTANCE OF THIN WALLED CYLINDRICAL SHELLS WITH AND WITHOUT A COMPLIANT ELASTIC CORE

The performance of a thin walled cylindrical shell with a compliant elastic core can be evaluated by comparing its buckling resistance to that of an empty shell of equal diameter and mass (Fig. 10). The outer cylindrical shells both have a density ρ , a Young's modulus E , and a Poisson's ratio v . The elastic core properties are: density ρ_c , Young's modulus E_c , and Poisson's ratio v_c . The elastic core has a central bore hole of radius b , removing the stress-free core material, and leaving a core thickness c equal to 1.6 times the buckling half wavelength. The thickness of the empty shell t_{eq} at equal mass is

$$t_{\text{eq}} = t \left[1 + \frac{c}{2t} \frac{\rho_c}{\rho} \left(2 - \frac{c}{a} \right) \right]. \quad (30)$$

Noting that $c = 5l/\pi = 5\lambda$ we obtain

$$t_{\text{eq}} = t \left[1 + 5 \frac{\lambda_{\text{cr}} \rho_c}{t \rho} \left(1 - 2.5 \frac{\lambda_{\text{cr}}/t}{a/t} \right) \right] \quad (31)$$

where, as before, λ_{cr} is the buckling wavelength for axisymmetric buckling under a uniaxial load (Fig. 4).

The ratio of the uniaxial buckling stress for the cylinder with the core to that without the core is then given by dividing eqn (9) by eqn (1) and setting the thickness of the empty cylinder equal to t_{eq} [eqn (31)]. We obtain, assuming $v = v_c = 0.3$,

$$\begin{aligned} \frac{\sigma_{\text{cr}}}{(\sigma_0)_{\text{eq}}} &= \frac{\frac{a/t}{10.9(\lambda_{\text{cr}}/t)^2} + \frac{(\lambda_{\text{cr}}/t)^2}{a/t} + 0.57 \frac{E_c}{E} \frac{a}{t} \frac{\lambda_{\text{cr}}}{t}}{0.605 \left[1 + 5 \frac{\lambda_{\text{cr}}}{t} \frac{\rho_c}{\rho} \left(1 - 2.5 \frac{\lambda_{\text{cr}}/t}{a/t} \right) \right]} \\ &= \frac{f_1}{0.605 \left[1 + 5 \frac{\lambda_{\text{cr}}}{t} \frac{\rho_c}{\rho} \left(1 - 2.5 \frac{\lambda_{\text{cr}}/t}{a/t} \right) \right]}. \end{aligned} \quad (32)$$

The uniaxial buckling load for the empty cylinder is found by multiplying the critical buckling stress [eqn (1)] by the shell area $2\pi a t_{\text{eq}}$. That for the cylinder with the core is found by multiplying the critical buckling stress by the shell area plus E_c/E times the core area. The resulting ratio of critical buckling loads with and without the core is (for $v = v_c = 0.3$)

$$\frac{P_{\text{cr}}}{(P_0)_{\text{eq}}} = \frac{\left[1 + 5 \frac{\lambda_{\text{cr}}}{t} \frac{E_c}{E} \frac{\rho_c}{\rho} \left(1 - 2.5 \frac{\lambda_{\text{cr}}/t}{a/t} \right) \right] f_1}{0.605 \left[1 + 5 \frac{\lambda_{\text{cr}}}{t} \frac{\rho_c}{\rho} \left(1 - 2.5 \frac{\lambda_{\text{cr}}/t}{a/t} \right) \right]^2}. \quad (33)$$

The ratio of critical buckling loads for uniaxial loading is plotted in Fig. 11. The plots have been made assuming that the ratio of the core to shell Young's moduli vary as the ratio of the core to shell density raised to a power of one or two, corresponding to a honeycomb or foam core supporting a shell made from the same solid material. Support of the shell by a core following $E_c/E = \rho_c/\rho$ leads to substantial increases in the axial buckling load, especially at large a/t . Support of the shell by a core following $E_c/E = (\rho_c/\rho)^2$ shows increases in the axial buckling load only for dense cores at high a/t .

The Brazier moment for a cylindrical shell with a compliant core is given by the second derivative of eqn (11) modified by eqns (25)–(27). Setting $v = v_c = 0.3$ we obtain the ratio of the Brazier moment for a cylindrical shell with a compliant core with a central bore hole to that of a hollow cylindrical shell of equal radius and mass:

$$\begin{aligned} \frac{M_{\text{Brazier}}}{(M_{\text{Brazier}})_{\text{eq}}} &= \frac{\left[1 + 1.747 \left(\frac{a}{t} \right)^3 \frac{E_c}{E} \frac{5\lambda_{\text{cr}}/t}{a/t} \left(2 - \frac{5\lambda_{\text{cr}}/t}{a/t} \right) \right]^{1/2}}{\left[1 + \frac{5\lambda_{\text{cr}}}{t} \frac{\rho_c}{\rho} \left(1 - \frac{5\lambda_{\text{cr}}/t}{2a/t} \right) \right]^2} \\ &\times \frac{\left[1 + \frac{5}{4} \frac{\lambda_{\text{cr}}}{t} \frac{E_c}{E} + 0.095 \frac{a}{t} \frac{E_c}{E} \left(1 - \left(1 - \frac{5\lambda_{\text{cr}}/t}{a/t} \right)^4 \right) \right]^{3/2}}{\left[1 + \frac{5}{4} \frac{E_c}{E} \frac{\lambda_{\text{cr}}}{t} \right]}. \end{aligned} \quad (34)$$

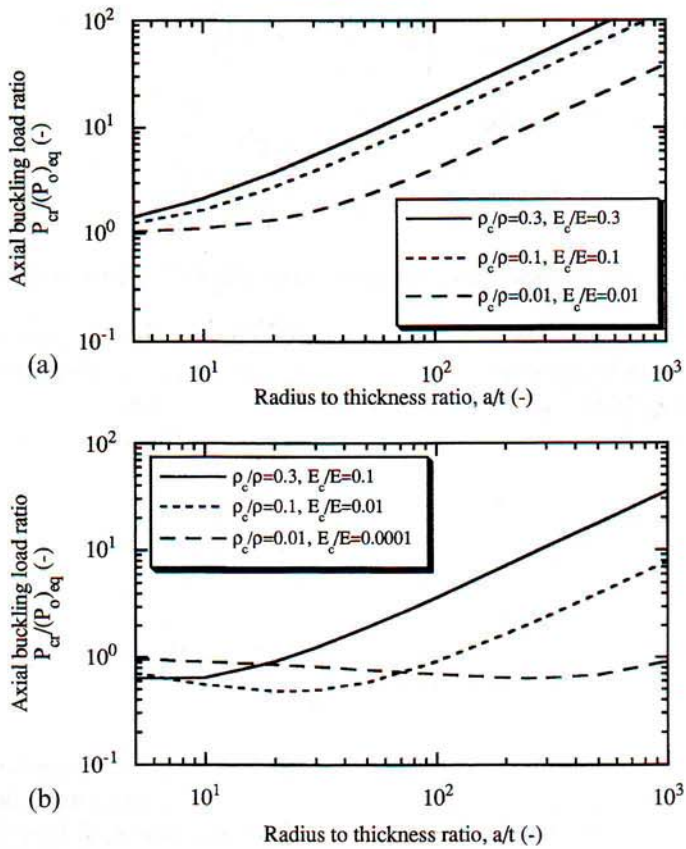


Fig. 11. The ratio of the elastic buckling load for uniaxial loading of a cylindrical shell with an elastic core to that without a core plotted against the ratio of shell radius to thickness for the shell with the core. (a) $E_c/E = \rho_c/\rho$; (b) $E_c/E = (\rho_c/\rho)^2$.

The ratio of Brazier moments is plotted in Fig. 12, again for cores obeying $E_c/E = \rho_c/\rho$ and $E_c/E = (\rho_c/\rho)^2$. The cores are much more effective in resisting Brazier buckling than uniaxial compression; both plots suggest an increase in Brazier moment of several fold for even the medium density core at $a/t > 20$. But in practice, local buckling precedes Brazier buckling, and it is the improvement in local buckling resistance that is most significant.

The ratio of the moments at which local buckling occurs for a cylindrical shell with and without a core is found from

$$\frac{M_{lb}}{(M_{lb})_{eq}} = \frac{\left(1 + 1.25 \frac{E_c \lambda_{cr}}{E t}\right) \left[1 + \frac{0.119 \frac{E_c \lambda_{cr}}{E t}}{1 + 1.25 \frac{E_c \lambda_{cr}}{E t}} - \frac{3}{2} \zeta\right] (1 - 3\zeta) f_1}{0.312 \left[1 + 5 \frac{\lambda_{cr}}{t} \frac{\rho_c}{\rho} \left(1 - 2.5 \frac{\lambda_{cr}/t}{a/t}\right)\right]^2 (1 - \zeta)} \quad (35)$$

where f_1 is given by eqn (9) and ζ by eqn (28) or Fig. 9, for $v = v_c = 0.3$. The ratio of the local buckling moments is plotted in Fig. 13, again for cores obeying $E_c/E = \rho_c/\rho$ and $E_c/E = (\rho_c/\rho)^2$. Cores following the linear relationship produce large increases in local buckling resistance, even for low relative densities and low ratios at a/t . Cores following the square relationship give rise to increases in local buckling resistance only at high relative densities.

Uniaxial compression and four point bending tests have been performed on silicone rubber cylindrical shells with and without a compliant core. The above analysis describes the results, detailed in the following, companion paper, well.

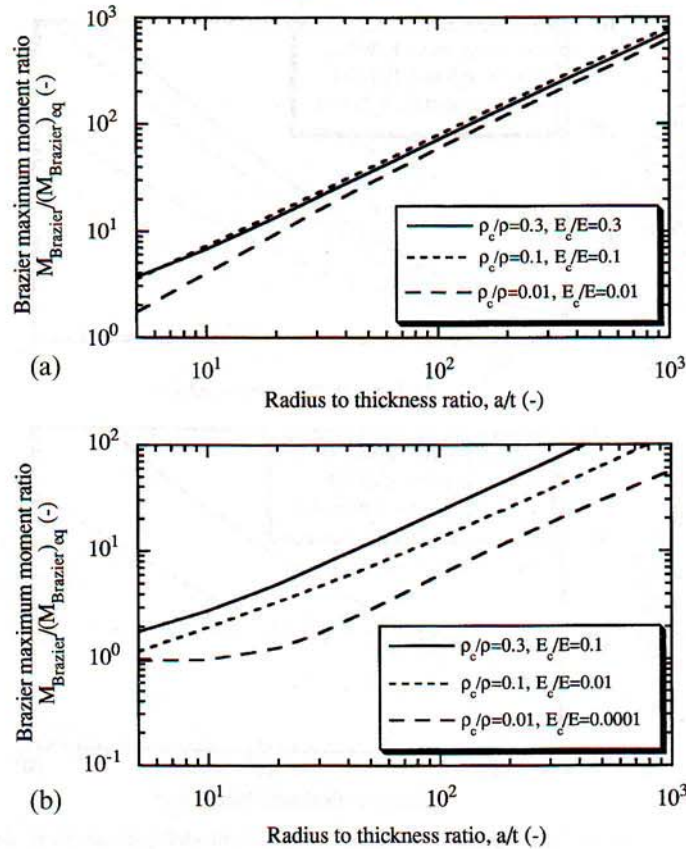


Fig. 12. The ratio of the Brazier moment for a cylindrical shell with an elastic core to that without a core plotted against the ratio of shell radius to thickness for the shell with the core. (a) $E_c/E = \rho_c/\rho$; (b) $E_c/E = (\rho_c/\rho)^2$.

5. IMPLICATIONS FOR ENGINEERING DESIGN: BIOMIMICKING

In nature, cylindrical shells are commonly stabilized by a compliant core. The theoretical analysis described here shows that the presence of a compliant core increases the buckling resistance in both axial compression and bending over that of a hollow cylinder of equal mass and radius. Honeycomb cores are more effective than foam cores. For the natural structures shown in Fig. 1, we estimate the increase to be a factor of between 1.5 and 4.

Cylindrical shells are used in a variety of engineering applications (Fig. 2). In practice, the measured elastic buckling loads are always less than the theoretical loads due to unavoidable geometric and material defects that cause premature loss of stability (Timoshenko and Gere, 1961; Kollár and Dulácska, 1984). In design elastic buckling loads are reduced by safety factors, termed “knock down” factors, to 30–40% of theoretical predictions (Kollár and Dulácska, 1984; Kenny, 1984). A compilation of published experimental results (Fig. 14) and more recent ones (see accompanying paper) show a consistent trend of cylinders with a compliant core achieving close to 100% of their theoretical strength as the core stiffness and the radius to thickness ratio increase. This difference in knock down factors further increases the elastic buckling resistance of cylinders with a compliant core relative to equivalent hollow cylinders.

In practice engineers stiffen cylindrical shells with longitudinal stringers or circumferential rings or both. The use of massive stiffeners, as in naval construction, offshore oil platforms and airframes, subdivides the shell into curved panels that are less sensitive to defects and achieve higher buckling loads (Timoshenko and Gere, 1961; Kenny, 1984). In some cases where high reliability is required, such as in aircraft design, the ribs supporting the shell may be designed to carry most of the external loads with the shell reduced to the role of an enclosure (Kollár and Dulácska, 1984). While this is a safe design, it requires

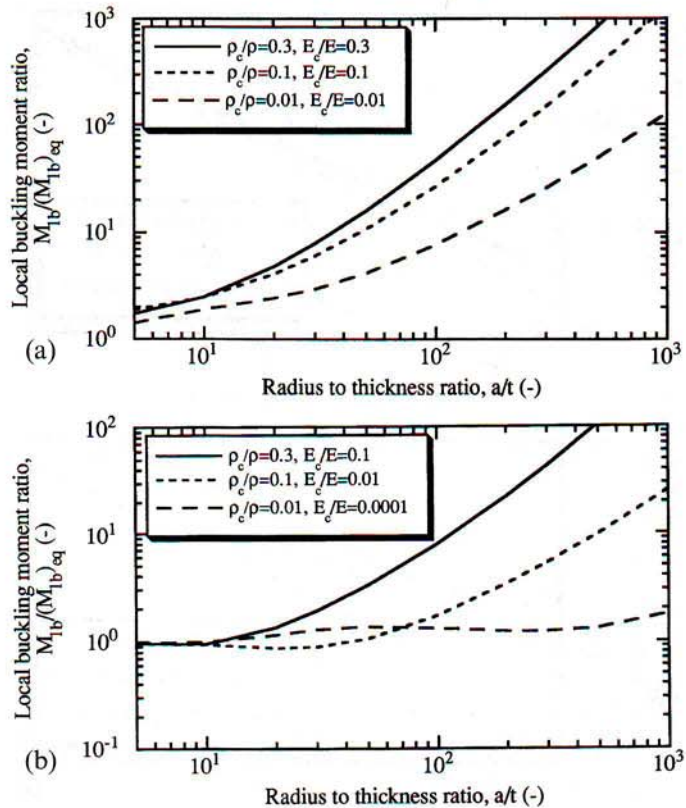


Fig. 13. The ratio of the local buckling moment of a cylindrical shell with an elastic core to that without a core plotted against the ratio of shell radius to thickness for the shell with the core. (a) $E_c/E = \rho_c/\rho$; (b) $E_c/E = (\rho_c/\rho)^2$.

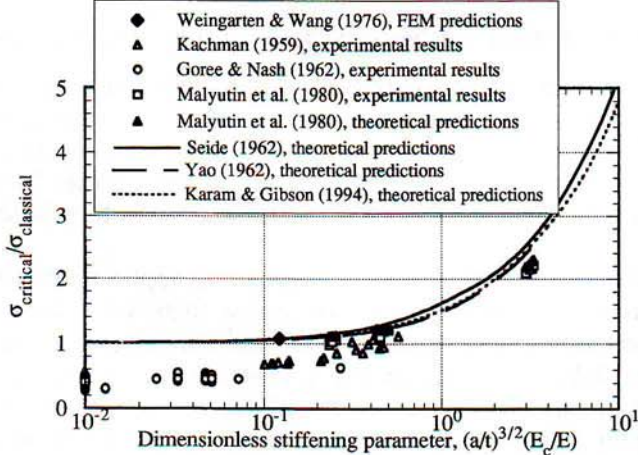


Fig. 14. Uniaxial compression buckling stress ratio σ_{cr}/σ_0 plotted against the dimensionless stiffening parameter $(a/t)^{3/2}(E_c/E)$ comparing our simplified analysis with the theoretical results of Seide (1962) and Yao (1962), the finite element analysis of Weingarten and Wang (1976) and data.

more material and is heavier than an unreinforced shell. A better way of reinforcing shells is with closely spaced longitudinal, circumferential or orthogonal stiffeners (Kollár and Dulácska, 1984); the close spacing of the stiffeners ensures that they buckle integrally with the skin. One or two way ribbed cylindrical shells exhibit the same types of buckling behavior as isotropic shells with the difference that the stiffeners increase the stretching and bending stiffnesses in the direction along which they are placed. Their buckling loads can be obtained by analyzing them as orthotropic shells.

For the case of buckling in axial compression and the associated local buckling problem in bending, theoretical investigations and experiments on near perfect ribbed shells have shown that ring stiffened cylinders always have a lower buckling load in axial compression than isotropic equivalent weight cylinders (Calladine, 1983; Tennyson, 1976). Stringer reinforced cylinders can be marginally more efficient (Tennyson, 1976). Ellinas and Croll (1981) and Ellinas *et al.* (1981) reached the same conclusions after an elaborate analysis. They, however, show that when imperfection sensitivity is taken into account, the improved knock down factors for circumferentially reinforced shells may reverse these conclusions for some stiffening ratios.

The thinner and deeper the stiffeners are, the higher the bending stiffness of the shell and hence the efficiency of the reinforcement. The depth of the stiffeners can be increased until local buckling of the stiffeners becomes the controlling failure mechanism. In the most general case an optimal reinforcing geometry would be one with both longitudinal and circumferential stiffeners equally distributed. The efficiency of this orthogonal reinforcement can be improved by making the stiffeners deeper and thinner, local buckling being prevented by the bracing provided by the closely spaced orthogonal elements. This optimisation scheme can be pursued until such a point where the orthogonal stiffening cannot buckle integrally with the shell, but instead becomes akin to a square honeycomb foundation stabilizing it. Honeycomb cores have Young's modulus proportional to density; their efficiency is given by the plots in Figs 11(a), 12(a) and 13(a).

Metal honeycombs, made by the expansion of adhesively bonded sheets of foil, have been widely used in lightweight structural sandwich panels in the aerospace industry. Recently, higher density metal honeycombs have been made by spot welding thicker sheets of material together. Metal foams are becoming more common; a low cost, 270kg/m^3 , closed cell aluminum foam is currently being tested by Alcan (Alcan International Ltd., Kingston, Ontario, Canada) and the Dnepropetrovsk Metallurgical Institute (DMI) in Ukraine is producing a range of metal honeycombs and foams (copper, iron, nickel, aluminum) with cell sizes from $10\ \mu\text{m}$ to 5 mm in relative densities from 0.3–0.9 (Walukas, 1992). The DMI materials can be made as laminates of alternating fully dense and cellular layers. Of particular interest, solid cylindrical shells with either a honeycomb or foam core can be produced as a single monolithic unit. The development of such engineering materials opens up the possibility of biomimicking of the natural structures shown in Fig. 1.

6. CONCLUSIONS

The simplified analysis of the buckling in axial compression of core filled cylindrical shells captures the most important elements of the full three-dimensional analysis and provides excellent analytical predictions in a tractable mathematical form. The axial buckling stress was used as a criterion for local buckling to develop a general solution for the elastic stability in pure bending of cylindrical shells with an elastic core including Brazier's ovalization and Poisson's ratio effects in the core. The analysis of stress decay in the core showed that the stresses in the core are negligible at a depth of roughly 1.6 half buckling wavelengths; the removal of core material beyond this depth does not affect the buckling stress of the shell. A parametric analysis showed that cylinders with this core depth have higher buckling loads than equivalent hollow cylinders.

The results of the analysis suggest that there is great potential for biomimicking of natural structures in engineering. A uniform honeycomb or foam foundation can become a more efficient substitute for stiffened shells; in addition to offering improved theoretical buckling resistance, shells with a compliant core offer reduced sensitivity to imperfections. The recent development of denser honeycomb materials, foamed metals and monolithic metal cylindrical shells with metal honeycomb or foam cores opens up the possibility of biomimicking of the natural structures shown in Fig. 1.

Acknowledgements—The analysis described in this paper benefitted from insightful discussions with Professor John Hutchinson of the Division of Applied Sciences, Harvard University. Financial support for this project was provided by the National Science Foundation (Grant Numbers MSS-9202202 and EID 9023692), for which we are grateful.

REFERENCES

- Akselrad, E. L. (1965). Refinement of the upper critical loading of pipe bending, taking into account the geometrical non-linearity. *Izv. Akad. Nauk. USSR, Otdelenie Tekhnicheskikh Nauk. Mech.* **4**, 123–139.
- Allen, H. G. (1969). *Analysis and Design of Structural Sandwich Panels*. Pergamon Press, Oxford.
- Almroth, B. O. and Brush, D. O. (1963). Postbuckling behaviour of pressure- or core-stabilized cylinders under axial compression. *AIAA J.* **1**, 2338–2341.
- Babich, I. Y. and Cherevko, M. A. (1984). Stability of cylindrical shells with an elastic-plastic filler under axial compression. *Prikl. Mekh.* **20**, 60–64.
- Bert, C. W. (1971). Buckling of axially compressed, core-filled cylinders with transverse shear flexibility. *J. Spacecraft* **8**, 546–548.
- Brazier, L. G. (1927). On the flexure of thin cylindrical shells and other thin sections. *Proc. R. Soc. London A* **116**, 104–114.
- Brush, D. O. and Almroth, B. O. (1962). Buckling of core-stabilized cylinders under axisymmetric external loads. *J. Aerospace Sci.* **29**, 1164–1170.
- Calladine, C. R. (1983). *Theory of Shell Structures*. Cambridge University Press, Cambridge.
- Ellinas, C. P. and Croll, J. G. A. (1981). Overall buckling of ring stiffened shells. *Proc. Inst. Civil Engr*, Part 2, **71**, 637–661.
- Ellinas, C. P., Batista, R. C. and Croll, J. G. A. (1981). Overall buckling of stringer stiffened cylinders. *Proc. Inst. Civil Engr*, Part 2, **71**, 479–512.
- Fabrik, O. (1977). Collapse of cylindrical elastic tubes under combined bending, pressure and axial loads. *Int. J. Solids Structures* **13**, 1257–1270.
- Fitzgibbon, D. P. (1960). Preliminary results of sub-scale tests on cylinders filled with an elastic core. Space Technology Laboratories, Inc. Los Angeles, CA, GM 60-7520, pp. 6–11.
- Gellin, S. (1982). A new class of solutions for buckling of a short cylindrical shell in pure bending. *Int. J. Mech. Sci.* **24**, 691–697.
- Goree, W. S. and Nash, W. A. (1962). Elastic stability of circular cylindrical shells stabilized by a soft elastic core. *Exp. Mech.* **2**, 142–149.
- Gough, G. J., Elam, C. F. and de Bruyne, N. A. (1940). The stabilization of a thin sheet by a continuous supporting medium. *J. R. Aero. Soc.* **44**, 12–43.
- Herrmann, G. and Forrestal, M. J. (1965). Buckling of a long cylindrical shell containing an elastic core. *AIAA J.* **3**, 1710–1715.
- Holston, A. (1967). Stability of inhomogeneous anisotropic cylindrical shells containing elastic cores. *AIAA J.* **5**, 1135–1138.
- Kachman, D. R. (1959). Test report on buckling of propellant cylinders under compressive loads. Space Technology Laboratories, Inc. Los Angeles, CA, GM 59-7520, pp. 6–24.
- Kenny, J. P. (1984). *Buckling of Offshore Structures*. Granada, London.
- Kollár, L. and Dulácska, E. (1984). *Buckling of Shells for Engineers*. Wiley, New York.
- Malyutin, I. S., Pilipenko, P. B., Georgievskii, V. P. and Smykov, V. I. (1980). Experimental and theoretical study of the stability in axial compression, of cylindrical shells reinforced with an elastic filler. *Prikl. Mekh.* **16**, 56–60.
- Myint, U. T. (1966). Stability of axially compressed core-filled cylinders. *AIAA J.* **4**, 552–553.
- Niklas, K. J. (1992). *Plant Biomechanics: An Engineering Approach to Plant Form and Function*. University of Chicago Press, IL.
- Reddy, B. D. and Calladine, C. R. (1978). Classical buckling of a thin-walled tube subjected to bending moment and internal pressure. *Int. J. Mech. Sci.* **20**, 641–650.
- Seide, P. (1962). The stability under axial compression and lateral pressure of circular-cylindrical shells with a soft elastic core. *J. Aerospace Sci.* **29**, 851–862.
- Seide, P. and Weingarten, V. I. (1961). On the buckling of circular cylindrical shells under pure bending. *J. Appl. Mech. ASME* **28**, 112–116.
- Seide, P. and Weingarten, V. I. (1962). Buckling of circular rings and long cylinders enclosing an elastic material under uniform external pressure. *Am. Rocket Soc. J.* **32**, 680–688.
- Stephens, W. B., Starnes, J. H. and Almroth, B. O. (1975). Collapse of long cylindrical shells under combined bending and pressure loads. *AIAA J.* **13**, 20–25.
- Tennyson, R. C. (1976). The effect of shape imperfections and stiffening on the buckling of circular cylinders. In *Buckling of Structures* (Edited by B. Budiansky), pp. 251–273. Springer-Verlag, NY.
- Timoshenko, S. P. and Gere, J. M. (1961). *Theory of Elastic Stability*, 2nd edition. McGraw-Hill, New-York.
- Vlasov, V. V. (1972). Stability of cylindrical shells containing a filler on being subjected to axial compression and external pressure. *Prikl. Mekh.* **9**(1), 117–121.
- Vlasov, V. V. (1975). Stability of composite shells with an elastic core. *Mekh. Polimerov* **3**, 544–547.
- Walukas, D. M. (1992). GASAR materials: a novel approach in the fabrication of porous materials. Internal Report USP Holdings, Ann Arbor, MI.
- Weingarten, V. I. and Wang, Y. S. (1976). Stability of shells attached to elastic core. *J. Engng Mech. Div. ASCE* **102**, 839–849.
- Yabuta, T. (1980). Effects of elastic supports on the buckling of circular cylindrical shells under bending. *J. Appl. Mech.* **47**, 866–870.
- Yao, J. C. (1962). Buckling of axially compressed long cylindrical shell with elastic core. *J. Appl. Mech.* **29**, 329–334.
- Yao, J. C. (1965). Bending due to ring loading of a cylindrical shell with an elastic core. *J. Appl. Mech.* **32**, 99–103.
- Zak, A. R. and Bolland, R. J. H. (1962). Elastic buckling of cylindrical thin shells filled with an elastic core. *Am. Rocket Soc. J.* **32**, 588–593.

APPENDIX

The total strain energy of the cylindrical shell with the compliant core is the sum of the strain energies of the hollow cylindrical shell and of the compliant core. The strain energy of the hollow cylindrical shell is the sum of the energy to ovalize the circular cross-section and that to bend the ovalized tube; it is given by eqn (21). The strain energy of the compliant core is the sum of the energy to ovalize the circular cross-section of the core, bend the ovalized core and to maintain the ovalized cross-section against Poisson ratio effects. Each of these terms is derived below. In calculating the strain energy terms we assume that the cylinder is long in comparison with its radius, producing plane strain conditions. We also assume that the cylindrical shell is much stiffer than the core so that it will fully restrain against Poisson ratio effects that tend to distort the core, i.e. the core will maintain the ovalized shape of the shell.

Strain energy associated with ovalization of compliant core

The radial and tangential displacements u and v , respectively, of a hollow cylindrical shell ovalized by ζ are (Calladine, 1983)

$$u = r\zeta \cos 2\theta \quad \text{and} \quad v = \frac{-r}{2}\zeta \sin 2\theta.$$

Assuming that the compliant core ovalizes to the same shape as the radial and circumferential strains, then

$$\begin{aligned}\varepsilon_r &= \partial u / \partial r = \zeta \cos 2\theta \\ \varepsilon_\theta &= \frac{u}{r} + \frac{\partial v}{r \partial \theta} = 0 \\ \gamma_{r\theta} &= \frac{\partial u}{r \partial \theta} + \frac{\partial v}{\partial r} - \frac{v}{r} = -2\zeta \sin 2\theta.\end{aligned}$$

The corresponding components of stress are

$$\begin{aligned}\sigma_r &= \frac{E_c}{(1+v_c)(1-2v_c)} [(1-v_c)\varepsilon_r + v_c\varepsilon_\theta] = \frac{(1-v_c)E_c}{(1+v_c)(1-2v_c)} \zeta \cos 2\theta \\ \sigma_\theta &= \frac{E_c}{(1+v_c)(1-2v_c)} [(1-v_c)\varepsilon_\theta + v\varepsilon_r] = \frac{vE_c}{(1+v_c)(1-2v_c)} \zeta \cos 2\theta \\ \tau_{r\theta} &= \frac{E_c}{2(1+v_c)} \gamma_{r\theta} = \frac{-E_c \zeta \sin 2\theta}{(1+v_c)}.\end{aligned}$$

The strain energy per unit length in the ovalized core is

$$U = \frac{1}{2} \int_0^{2\pi} \int_0^a (\sigma_r \varepsilon_r + \sigma_\theta \varepsilon_\theta + \tau_{r\theta} \gamma_{r\theta}) r dr d\theta.$$

Substituting for the stresses and strains we obtain

$$U = \frac{\pi E_c \zeta^2 a^2}{4} \frac{(3-5v)}{(1+v_c)(1-2v_c)}.$$

Strain energy associated with bending of the core filled cylinder

The strain energy per unit length to bend a member of flexural rigidity EI to a curvature C is

$$U = \frac{1}{2} EI C^2.$$

For a hollow tube with ovalization ζ the moment of inertia is (Calladine, 1983)

$$I = \pi a^3 t \left(1 - \frac{3}{2}\zeta + \frac{5}{8}\zeta^2\right)$$

and for a circular shell filled with a compliant core of modulus E_c this becomes

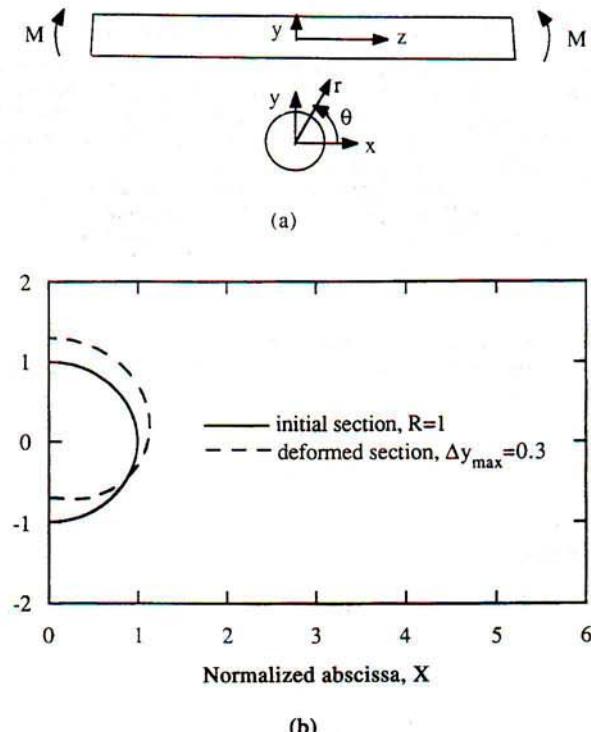


Fig. A1. (a) A beam of circular cross-section in pure bending with coordinate axes defined; (b) the distortion of the circular cross-section of the beam due to Poisson's ratio effects.

$$I = \left(\pi a^3 t + \frac{\pi a^4}{4} \frac{E_c}{E} \right) \left(1 - \frac{3}{2} \zeta + \frac{5}{8} \zeta^2 \right) = \pi a^3 t \left(1 + \frac{E_c}{E} \frac{a}{4t} \right) \left(1 - \frac{3}{2} \zeta + \frac{5}{8} \zeta^2 \right).$$

Strain energy associated with Poisson's ratio effects due to bending

Here we calculate the radial and circumferential strains that would be induced in a beam of circular cross-section deforming freely in pure bending (Fig. A1). We then calculate the strain energy required to maintain the circular cross-section.

The strain in the longitudinal (*z*) direction is simply

$$\varepsilon_z = -Cy = -Cr \sin \theta$$

while the strains in the radial and circumferential directions are

$$\varepsilon_r = \varepsilon_\theta = -v_c \varepsilon_z = v_c Cr \sin \theta.$$

Noting that

$$\varepsilon_r = \frac{\partial u}{\partial r}$$

and

$$\varepsilon_\theta = \frac{u}{r} + \frac{1}{r} \frac{\partial v}{\partial \theta},$$

we find

$$u = \frac{v_c}{2} Cr^2 \sin \theta \quad \text{and} \quad v = -\frac{v_c}{2} Cr^2 \cos \theta.$$

Substituting in

$$\gamma_{r\theta} = \frac{1}{r} \frac{\partial u}{\partial \theta} + \frac{\partial v}{\partial r} - \frac{v}{r}$$

gives

$$\gamma_{r\theta} = -v_c Cr \cos \theta.$$

The strain energy per unit length of cross-section to maintain the circular cross-section is then (noting that $\varepsilon_r = \varepsilon_\theta$ and $\sigma_r = \sigma_\theta$)

$$\begin{aligned} U &= \frac{1}{2} \int_0^a \int_0^{2\pi} (2\sigma_r \varepsilon_r + \tau_{r\theta} \gamma_{r\theta}) r d\theta dr \\ &= \frac{1}{2} \int_0^a \int_0^{2\pi} \left(\frac{2v_c^2 E_c C^2 r^2 \sin^2 \theta}{(1+v_c)(1-2v_c)} + \frac{v_c^2 E_c C^2 r^2 \cos^2 \theta}{2(1+v_c)} \right) r d\theta dr \\ &= \frac{\pi}{16} \frac{v_c^2 (5-2v_c)}{(1+v_c)(1-2v_c)} E_c C^2 a^4. \end{aligned}$$